

## ANALYZE OF SUNFLOWER OIL INCORPORATION IN POLY(ACRYLIC ACID)/ CHITOSAN SPONGES USING THIN PLATE SPLINE INTERPOLATION METHOD

---

***Talita Goulart da Silva***

Programa de Pós-graduação em Engenharia Química, Universidade Federal Rural do Rio de Janeiro, Seropédica, RJ  
<http://lattes.cnpq.br/1271187450832634>  
<https://orcid.org/0000-0001-8170-5528>

***Tiago dos Santos Mendonça***

Programa de Engenharia Metalúrgica de Materiais, COPPE, Universidade Federal do Rio de Janeiro, Rio de Janeiro, RJ  
<http://lattes.cnpq.br/1049467790434761>  
<https://orcid.org/0000-0001-7568-4193>

***Raquel de Souza Ribeiro***

Programa de Pós-graduação em Engenharia Química, Universidade Federal Rural do Rio de Janeiro, Seropédica, RJ.  
<https://lattes.cnpq.br/4950904629435561>  
<https://orcid.org/0000-0003-2178-2868>

***Cristiane Evelise Ribeiro da Silva***

Divisão de Materiais – Instituto nacional de Tecnologia, 3DMatCIS, Rio de Janeiro, RJ  
<http://lattes.cnpq.br/6945452534442737>  
<https://orcid.org/0000-0003-4855-2579>

All content in this magazine is licensed under a Creative Commons Attribution License. Attribution-Non-Commercial-Non-Derivatives 4.0 International (CC BY-NC-ND 4.0).



**Sonia Letichevsky**

Departamento de Engenharia Química e de  
Materiais - Pontifícia Universidade Católica  
do Rio de Janeiro,  
Rio de Janeiro, RJ  
<http://lattes.cnpq.br/6948246729078101>  
<https://orcid.org/0000-0003-1419-7935>

**Roberta Helena Mendonça**

Programa de Pós-graduação em Engenharia  
Química, Universidade Federal Rural do Rio  
de Janeiro, Seropédica, RJ  
<http://lattes.cnpq.br/3724636742992170>  
<https://orcid.org/0000-0003-1034-7027>

**Abstract:** Chitosan/PAA sponges (potential applied in wound healing) were produced and loaded with serum and Dersani<sup>®</sup>. Thin Plate Spline interpolation method (TPSIM) was used to evaluate the effect of composition and the time in the sponges capability of fluid incorporation. A surface composed of experimental and interpolated data were obtained. polynomial regression with multiple independent variables was used to evaluate the contribution of each variable. Scanning electron microscopy (MEV), x-Ray diffraction (XRD) and Differential Scanning Calorimetry (DSC) were done. The composition affects the sponge's morphology. Material amorphization occurred due chitosan/PAA interaction as stated by DSC and XRD. TPSIM showed that the composition has a significantly greater individual contribution in fluid absorption. The time individually contribution is small. However, the interaction between time and composition are responsible for the non-linear shape of the curve and have relevant impact in fluid incorporation.

**Keywords:** wound dressing, modelling, biomaterial, sponge

## INTRODUCTION

Chitosan (Chi) sponges has been considered in the treatment of wound dressing. Poly (acrylic acid) (PAA), is a synthetic and hydrophilic polymer. [1] It has been used as a gelling agent in drugs and for the synthesis of hydrogels. [2] Mixtures of chitosan and PAA have been used in the controlled release of drugs. [3]

Dersani<sup>®</sup> oil is composed of triglycerides of capric and caprylic acids, clarified sunflower oil, lecithin, retinol palmitate, tocopherol acetate, and alpha-tocopherol. This oil has been used in the treatment of wounds. [4], [5]

Thin plate spline interpolation method (TPSIM) is used to approximate a smooth, continuous surface from a set of scattered data

points. The TPSIM basis function is given by the Equation 1. [6]

$$\phi_{(r)} = r^2 \times \log(r) \quad (1)$$

where  $r$  is the Euclidean distance between a data point and a control point. The interpolant is then defined as Equation 2 shows [7]

$$f_{(x,y)} = a_0 + a_1 \times x + a_2 \times y + \sum \phi_{(r)} \times w_i \quad (2)$$

where  $a_0$ ,  $a_1$ , and  $a_2$  are constants and  $w_i$  are weights assigned to each control point.

One advantage of the TPSIM is that it provides a smooth interpolation surface that passes through all the data points, while avoiding overfitting or oscillations. [8], [9] This method was used to calculate and estimate the torque values through rheometric tests and to evaluate the effect of parameters layer thickness, [10] deposition speed and printing direction on tensile properties and dimensional accuracy of PLA 3D printed parts. [11]

The aim of this work was studied the mass variation (MV) of chitosan/ PAA in Dersani® oil and physiological saline solution using the TPSIM was used to evaluate the effect of time and composition in the fluid absorption.

## EXPERIMENTAL

### PRODUCTION OF CHITOSAN/PAA SPONGES

PAA (Sigma-Aldrich  $M_v \sim 4,000,000$ ) solution (2 wt % in water) and Chi (Sigma-Aldrich - low molecular weight, degree of deacetylation: 75%) solution (2 wt % in acetic acid solution 0.5% v/v) were mixed in the proportions (Chi: PAA (% v/v)) 10:90; 25:75; 50:50; 75:25 and 100:0). The mixtures were lyophilized using the equipment LIOTOP, model L 101. The samples were named as  $S_i$  where  $i$  refers to the amount (v/v %) of chitosan in the samples:  $S_0$  (100 v/v % PAA),

$S_{10}$  (10 v/v % chitosan – 90 v/v % PAA),  $S_{25}$  (25 v/v % chitosan – 75 v/v % PAA),  $S_{50}$  (50 v/v % chitosan – 50 v/v % PAA),  $S_{75}$  (75 v/v % chitosan – 25 v/v % PAA) e  $S_{100}$  (100 v/v % chitosan).

## CHARACTERIZATION

The samples were analyzed by Scanning electron microscopy (SEM) using a microscope (HITACHI, TM3000 model, Tokyo, Japan); by X-Ray Diffraction (XRD) using a diffractometer (Mini Flex II, Rigaku, Tokyo, Japan) operating with a  $CuK\alpha$  source ( $\lambda = 1.542 \text{ \AA}$ ), the scans range were  $2\theta = 6-60^\circ$ , with a scan speed of  $2^\circ \cdot s^{-1}$ , and by Differential scanning calorimetry (DSC) using a Perkin-Elmer Simultaneous Thermal Analyzer 6000. Samples were heated from room temperature to  $700^\circ C$  at  $10^\circ C \cdot min^{-1}$  under  $N_2$  at a flow rate of  $20 \text{ mL} \cdot min^{-1}$ .

### TPSIM AND POLYNOMIAL FITTING – FLUID INCORPORATION STUDY

The samples were immersed, separately, in serum and oil (Dersani®) for 140 minutes. The MV values were calculated using Equation (3), where  $M_t$  is the mass of the samples at time  $t$ , and  $M_0$  is the mass of the dry samples.

$$MV = \left( \frac{M_t - M_0}{M_0} \right) \times 100 \quad (3)$$

TPSIM was performed, based in the MV values obtained by Equation (3), using the software MATLAB®. Polynomial fit p55, Equation (4), was applied simultaneously to the experimental and the interpolated data to obtain a 3D surface that correlates MV, composition, and time, Equation (3). [10], [11]

$$\sum_{n,m}^{(n,m) \in \mathbb{N}^2, n+m \leq 5} p_{mn} x^m y^n, \quad (4)$$

where  $[p]_{nm}$  is the matrix with the

summation coefficients.

In this work,  $f(x, y)$  is the *MV*,  $x$  is the composition of the sponges (represented by the mass percentage of chitosan in the sample), and  $y$  is the time. According to Equation (4), it is important to note that:

1. If  $n = 0$  and  $m > 0$ , the term of the polynomial ( $p_{mn}$ ) only depends on the variable  $x$  (composition);
2. If  $m = 0$  and  $n > 0$ , the term of the polynomial ( $p_{mn}$ ) only depends on the variable  $y$  (time);
3. If  $n > 0$  and  $m > 0$ , the polynomial term ( $p_{mn}$ ) shows the interaction between the  $x$  and  $y$ .

Polynomial coefficients can be represented according to the matrix  $[p]_{nm}$ , highlighting the coefficients that depend only on time (blue) and on concentration (red).

$$\begin{bmatrix} p_{00} & p_{01} & p_{02} & p_{03} & p_{04} & p_{05} \\ p_{10} & p_{11} & p_{12} & p_{13} & p_{14} & p_{15} \\ p_{20} & p_{21} & p_{22} & p_{23} & p_{24} & p_{25} \\ p_{30} & p_{31} & p_{32} & p_{33} & p_{34} & p_{35} \\ p_{40} & p_{41} & p_{42} & p_{43} & p_{44} & p_{45} \\ p_{50} & p_{51} & p_{52} & p_{53} & p_{54} & p_{55} \end{bmatrix}$$

## RESULTS AND DISCUSSION

The sponges were characterized by XRD (Figure 1).  $S_0$ ,  $S_{10}$  and  $S_{25}$  patterns were similar to pure PAA diffractogram. The samples  $S_{50}$  and  $S_{75}$  did not present characteristic peaks of PAA and / or chitosan. This result indicates a strong interaction between these polymers. DSC results (Figure 2) indicate the amorphization of the sample since PAA's and Chitosan's peaks were not observed in  $S_{75}$ . The only thermal event observed (around 100 °C) is related to water loss. Composition also affects sponges' morphology and pore size (Figure 3). As the chitosan content increases, fibrillar structures can be observed.

TPSIM was applied to obtain a surface (Figure 3) composed for the real data (Equation 1) and the interpolated data.

When performing polynomial regression with multiple independent variables, the regression coefficients can be used to indicate the contribution of each variable. Analyzing the coefficients associated with the individual contributions (indicated in the matrix  $pSO$  [nm] and  $pS$  [nm]), we observed that the composition has a significantly greater individual contribution to the behavior of the curve. Although time individually contribute is of little significance, the mixed coefficients (interaction between time and composition),  $p_{mn}$  when  $p \neq n$ , are responsible for the non-linear shape of the curve and have relevant magnitudes.

A minimum point between 40 and 60 min was observed (Figure3). The compression between the polymer chains and increase in the *MV* value can be related to polymer chain relaxation and fluid absorption. The slow reorientation of polymer molecules can lead to a wide variety of anomalous effects for both permeation and absorption [12]–[14] These results agree with SEM, XRD and DSC analyses which can explain the behavior of samples with chitosan amount greater than 50%. Samples, with a higher proportion of PAA presents negative *MV* values, probably due the mechanical strength of the material.

To corroborate the information obtained by TPSIM analysis (Figure 3 and related matrices) the *MV* data were statistically analyzed. The analysis of ANOVA-2-way variance was performed, with 2 factors, composition (5 levels,  $S_{10}$ ,  $S_{25}$ ,  $S_{50}$ ,  $S_{75}$  and  $S_{100}$ ) and time (5 levels, 30 min, 50 min, 110 min, 24 h and 7 days). It was possible to observe that the composition affects the amount of oil and serum absorbed ( $p < 0.05$ ). The Tukey's test verified that the difference was significant ( $p < 0.05$ ). Furthermore, this study exhibited better absorption performance then the wound dressings reviewed in Fulton's et al. [15]

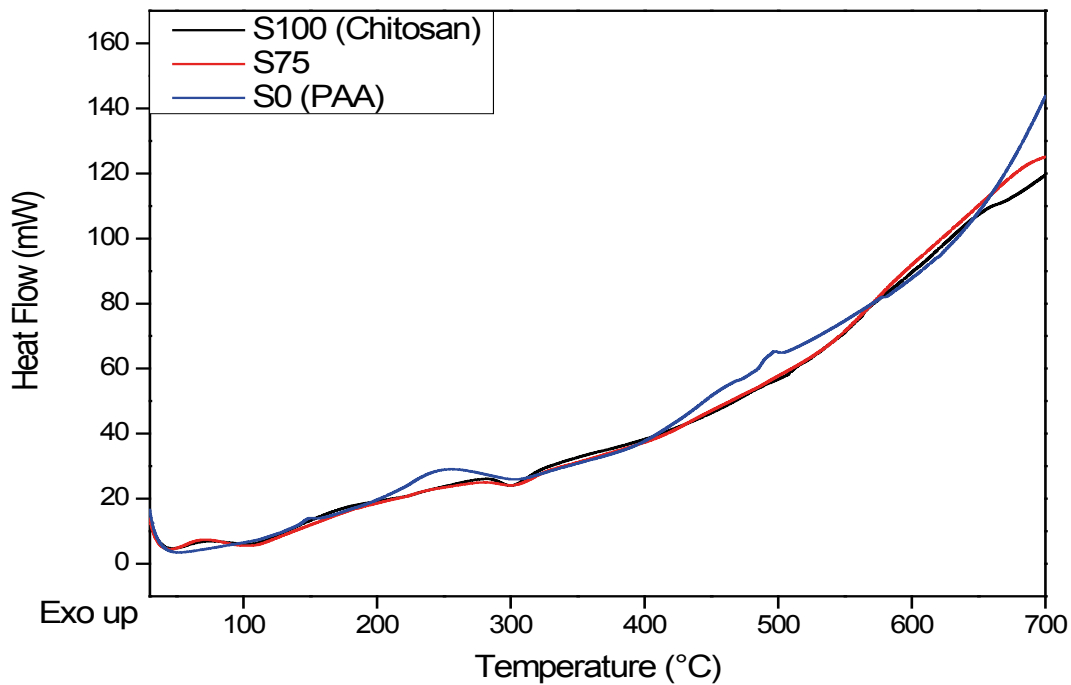


Figure 1. DSC curves of Chitosan, PAA and  $S_{75}$  sample

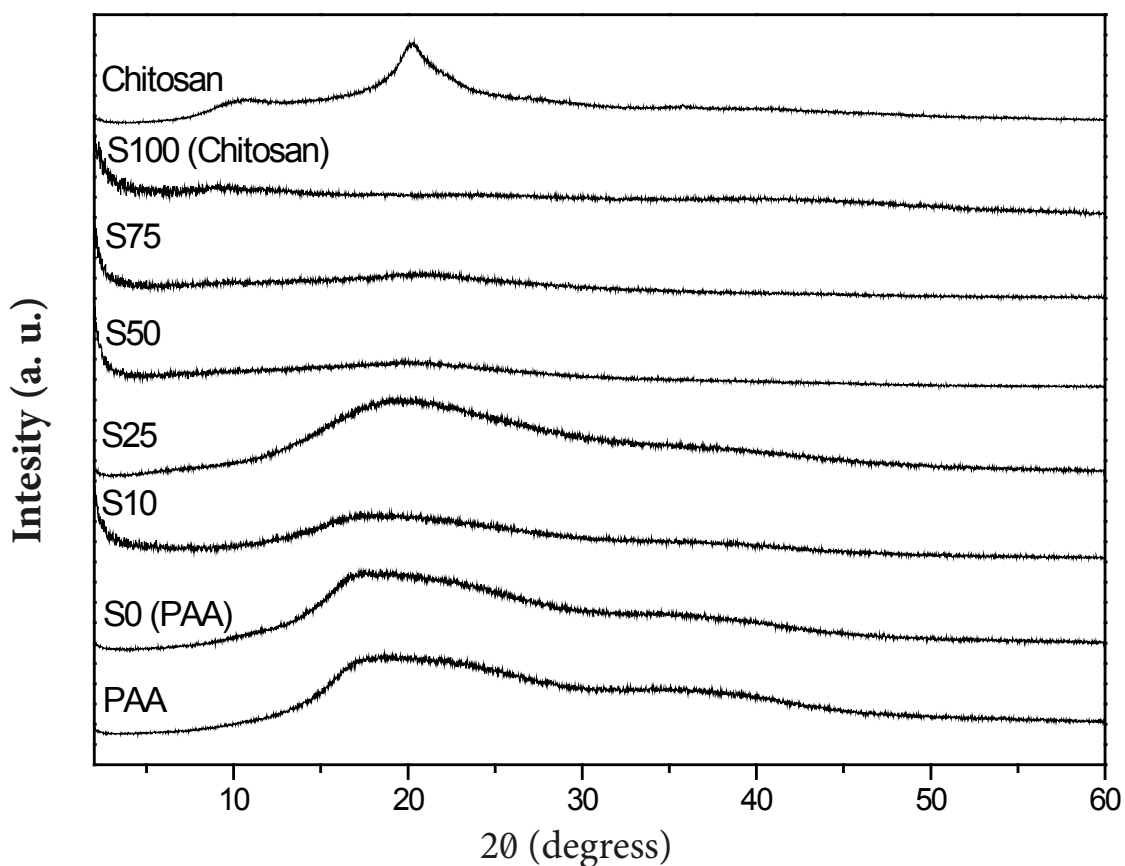
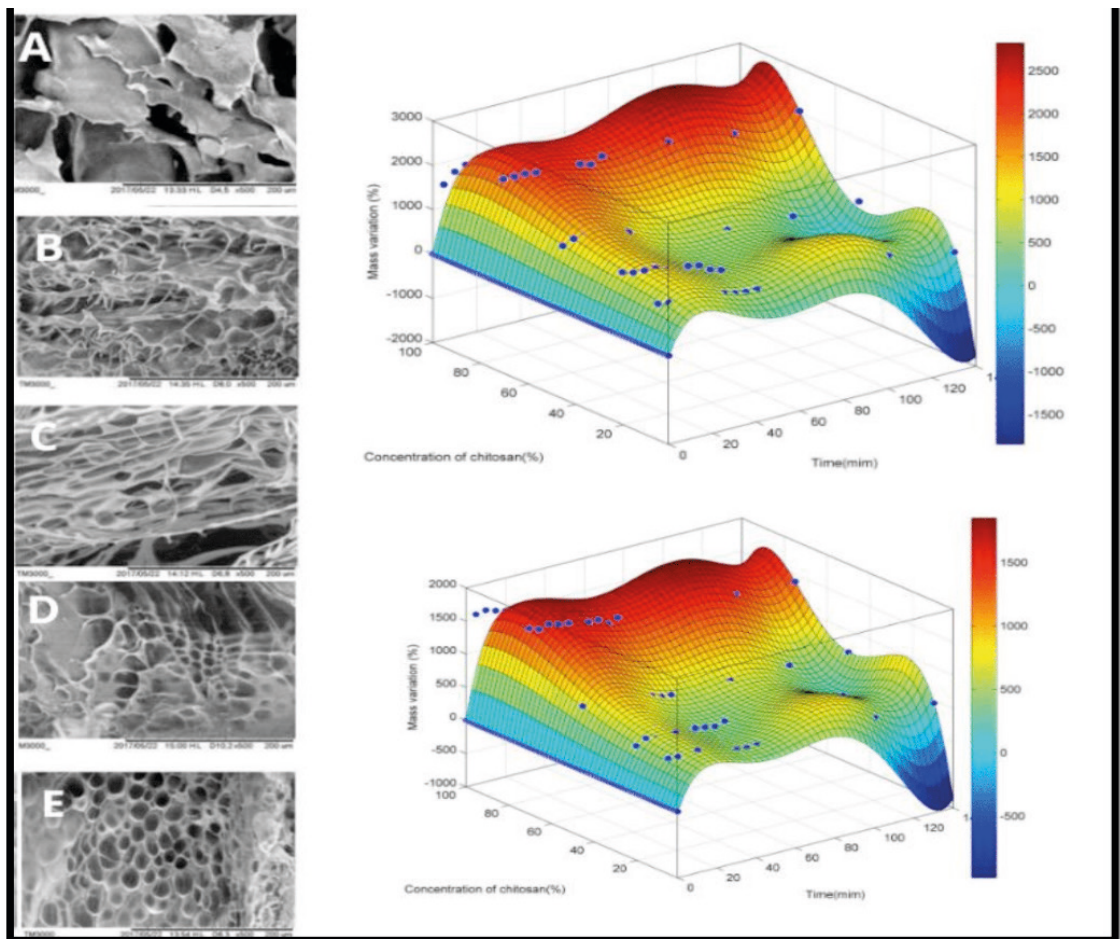


Figure 2. Diffractograms of Chitosan, PAA and  $S_i$  samples

$$[p]_{mn} = \begin{pmatrix} -2,29^{-19} & 6,15^{-18} & 3,24^{-17} & 5,76^{-17} & -2,30^{-17} & -1,42^{-17} \\ 12200 & 35378 & -139297 & 364403,2 & -294958 & 0 \\ -63610 & -46942 & -21599,2 & 55017,2 & 0 & 0 \\ 121900 & 48468 & -22148 & 0 & 0 & 0 \\ -98410 & -9590 & 0 & 0 & 0 & 0 \\ 27710 & 0 & 0 & 0 & 0 & 0 \end{pmatrix}$$

$$[p]_{mn} = \begin{pmatrix} 1,70^{-17} & -4,38^{-17} & -1,73^{-15} & 9,13^{-15} & -1,50^{-14} & 7,81^{-15} \\ 8098 & 10488,8 & -32908,4 & 162307,6 & -156775,696 & 0 \\ -38920 & -26782 & -52508,4 & 54303,76 & 0 & 0 \\ 75770 & 42126 & -6411,16 & 0 & 0 & 0 \\ -63300 & -11954,6 & 0 & 0 & 0 & 0 \\ 18430 & 0 & 0 & 0 & 0 & 0 \end{pmatrix}$$



**Figure 3.** SEM images of (A) S<sub>10</sub> (B) S<sub>25</sub> (C) S<sub>50</sub> (D) S<sub>75</sub> (E) S<sub>100</sub> (left), mass variation S<sub>1</sub> samples in physiological solution (up right) and mass variation of S<sub>1</sub> samples in sunflower oil (down right)

## CONCLUSIONS

PAA/Chi sponges, with different proportions, were produced by lyophilization. XRD and DSC analysis indicates a stronger interaction between PAA and chitosan. According to TPSIM the composition has a significantly greater individual contribution

to fluid absorption. The time individual contribution is of little significance significantly, the mixed coefficients (interaction between time and composition) are responsible for the non-linear shape of the curve and have relevant impact in fluid incorporation as corroborate by ANOVA.

## REFERENCES

- [1] M. Sukul *et al.*, "In vitro biological response of human osteoblasts in 3D chitosan sponges with controlled degree of deacetylation and molecular weight," *Carbohydr Polym*, vol. 254, p. 117434, Feb. 2021, doi: 10.1016/J.CARBPOL.2020.117434.
- [2] X. Du *et al.*, "Microchannelled alkylated chitosan sponge to treat noncompressible hemorrhages and facilitate wound healing," *Nat Commun*, vol. 12, no. 1, p. 4733, Aug. 2021, doi: 10.1038/s41467-021-24972-2.
- [3] M. Y. Abdelaal, M. S.I. Makki, and T. R.A. Sobahi, "Modification and Characterization of Polyacrylic Acid for Metal Ion Recovery," *American Journal of Polymer Science*, vol. 2, no. 4, pp. 73–78, Aug. 2012, doi: 10.5923/j.ajps.20120204.05.
- [4] M. C. García *et al.*, "Bioadhesive and biocompatible films as wound dressing materials based on a novel dendronized chitosan loaded with ciprofloxacin," *Carbohydr Polym*, vol. 175, pp. 75–86, Nov. 2017, doi: 10.1016/J.CARBPOL.2017.07.053.
- [5] L. Y. Zakharova *et al.*, "The polyacrylic acid/modified chitosan capsules with tunable release of small hydrophobic probe and drug," *Colloids Surf A Physicochem Eng Asp*, vol. 471, pp. 93–100, Apr. 2015, doi: 10.1016/J.COLSURFA.2015.02.016.
- [6] F. L. Bookstein, "Principal warps: thin-plate splines and the decomposition of deformations," *IEEE Trans Pattern Anal Mach Intell*, vol. 11, no. 6, pp. 567–585, Jun. 1989, doi: 10.1109/34.24792.
- [7] Amos Gilat and Vish Subramaniam, *Métodos Numéricos para Engenheiros e Cientistas: Uma Introdução com Aplicações Usando o MATLAB*. Bookman Editora, 2008.
- [8] M. Guidoni *et al.*, "Development and evaluation of a vegetable oil blend formulation for cutaneous wound healing," *Arch Dermatol Res*, vol. 311, no. 6, pp. 443–452, Aug. 2019, doi: 10.1007/s00403-019-01919-8.
- [9] A. L. Mohamed and A. G. Hassabo, "Composite material based on pullulan/silane/ZnO-NPs as pH, thermo-sensitive and antibacterial agent for cellulosic fabrics," *Advances in Natural Sciences: Nanoscience and Nanotechnology*, vol. 9, no. 4, p. 045005, Nov. 2018, doi: 10.1088/2043-6254/aaee0.
- [10] T. B. Cubiça *et al.*, "INCORPORATION AND RELEASE OF HAMAMELIS VIRGINIANA IN 'SCAFFOLDS' PRECURSOR MATRIX: AN APPROACH WITH THE 'THIN PLATE SPLINE' INTERPOLATION METHOD," *REVISTA FOCO*, vol. 16, no. 02, p. e921, Feb. 2023, doi: 10.54751/revistafoco.v16n2-060.
- [11] P. H. M. Cardoso *et al.*, "Mechanical and dimensional performance of poly(lactic acid) 3D-printed parts using thin plate spline interpolation," *J Appl Polym Sci*, vol. 137, no. 39, p. 49171, Oct. 2020, doi: 10.1002/app.49171.
- [12] J. Ge, F. Wang, X. Yin, J. Yu, and B. Ding, "Polybenzoxazine-Functionalized Melamine Sponges with Enhanced Selective Capillarity for Efficient Oil Spill Cleanup," *ACS Appl Mater Interfaces*, vol. 10, no. 46, pp. 40274–40285, Nov. 2018, doi: 10.1021/acsami.8b14052.
- [13] S. Chatterjee, P. Doshi, and G. Kumaraswamy, "Capillary uptake in macroporous compressible sponges," *Soft Matter*, vol. 13, no. 34, pp. 5731–5740, 2017, doi: 10.1039/C7SM00826K.
- [14] D. Vandevoorde, M. Pamplona, O. Schalm, Y. Vanhellefont, V. Cnudde, and E. Verhaeven, "Contact sponge method: Performance of a promising tool for measuring the initial water absorption," *J Cult Herit*, vol. 10, no. 1, pp. 41–47, Jan. 2009, doi: 10.1016/J.CULHER.2008.10.002.
- [15] J. A. Fulton *et al.*, "Wound Dressing Absorption," *Adv Skin Wound Care*, vol. 25, no. 7, pp. 315–320, Jul. 2012, doi: 10.1097/01.ASW.0000416003.32348.e0.